JOURNAL OF MAGNETIC RESONANCE **125,** 355–357 (1997)
ARTICLE NO. MN971121

''Negative Edge Enhancement'' in NMR Imaging with Diffusion at Permeable Susceptibility Interfaces

NIKOLAUS NESTLE,* KAY RYDYGER, AND RAINER KIMMICH

Universität Ulm, Sektion Kernresonanzspektroskopie, D-89069 Ulm, Federal Republic of Germany

Received October 18, 1996; revised January 8, 1997

As a consequence of the strong field gradients required for extreme spatial resolution, the contrasts in NMR micrographs tend to be diffusion weighted (*1–6*). Recently, edge enhancement effects in liquid-filled capillaries were described and analyzed by several researchers (*1–3, 5*). These phenomena are due to the restriction of the random walks of diffusing particles by impermeable walls. The perpendicular diffusive displacement of molecules in the vicinity of the walls is smaller than in the bulk liquid. If bipolar gradients, such as the read gradient with its refocusing part, are used, the echo attenuation due to diffusive movement in gradient direction is therefore smaller for spins close to a wall than for those in the bulk liquid. That is, ordinary edge enhancement effects are caused by variations of the diffusive propagator due to partially reflecting walls or spatially varying diffusion coefficients. In Ref. (*4*), there is also an account of varied diffusive attenuation due to additive or subtractive superposition of the imaging gradient and stray gradients produced by an impermeable object of different susceptibility in the sample.

In this contribution, by contrast, observations of diffusion artifacts in samples with a spatially nearly uniform diffusive propagator are presented: such samples can be produced from polyelectrolyte gels. The effect was first observed with tubes of Ca alginate during ion-exchange experiments with light rare-earth ions. The preparation and the properties of the samples used in these experiments are discussed in detail in Refs. (*7–11*). The properties most important for this context are: (i) Due to their magnetic moments, most rare-earth ions are paramagnetic. For some ion species such as Pr^{3+} and Nd^{3+}, the relaxation times of alginate gels bound to these ions are relatively long so that there is still an appreciable signal intensity from the respective regions of the sample at short echo times. (ii) Most rare-earth ions have been found to intrude into alginate gels with a steep reaction front (see Figs. 1 and 2, Refs. (*8, 10, 11*). (iii) Neither the edges of the alginate objects nor the reaction fronts perceptibly affect the short-time water diffusion coefficients (*12*).

* Present address: MPI für Festkörperforschung, Heisenbergstraße 1, D-70569 Stuttgart.

In the absence of the diffusion effects to be discussed here, one would expect a susceptibility shift artifact. A simulation is shown in Fig. 3. In addition to such shift artifacts, diffusion produces a symmetrical dark ring structure along the boundary between the Pr-loaded and the unloaded alginate region. This can be seen in Fig. 4. This ''negative edge enhancement'' was observed in several hundred images of ion-exchange processes envolving different species of light rare-earth ions. Only in experiments with Yb^{3+} ions where the intrusion front is much smoother, the artifact was found to be very faint and smeared out.

In order to corroborate this observation, further experi-

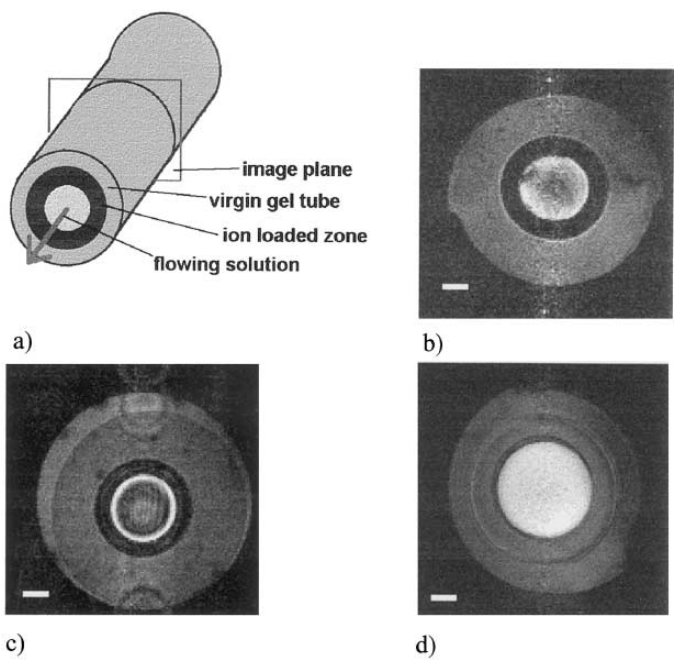

FIG. 1. NMR imaging of ion exchange in Ca-alginate tubes: (a) experimental setup, (b) cross section of an alginate tube after 7 h exposure to 1 m*M* Gd^{3+}, T_E = 11 ms, (c) after 7 h to 1 m*M* Nd^{3+}, T_E = 20 ms, (d) after 13 h to 1 m*M* Pr^{3+}, T_E = 7 ms. Note the sharp reaction fronts in all images. Other image parameters: gradient-echo sequence with T_R = 250 ms, 1 mm slice thickness, and (75 μm)^2 in plane resolution, 128 × 128 pixels. The bright bar corresponds to 1 mm. For further experimental details, see (*8, 10, 11*).

1090-7807/97 $25.00

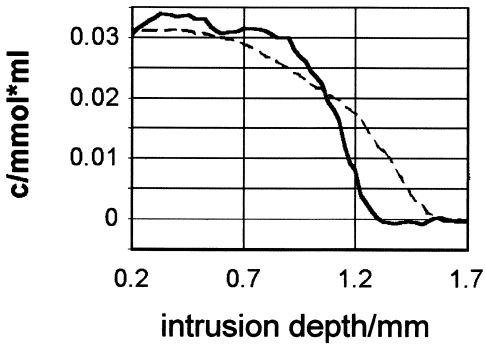

FIG. 2. Concentration profiles evaluated from quantitative susceptibility images [see (*10, 11*)] for Pr^{3+} ions (solid curve) and Yb^{3+} ions (dashed curve). The concentration profile for the Pr ions is probably even steeper than the graph suggests; the front is spoiled by diffusion and shift artifacts which have not been fully corrected.

ments with a ''static'' sample without reactions and flow were performed: This sample consisted of a Ce-alginate cylinder immersed in pure water (Fig. 5). It is known that for short diffusion times in polyelectrolyte gels with high water content, the diffusion coefficients are only slightly lower than those in free water (*12*). That is, a susceptibility step occurs but no diffusion barrier.

The negative edge enhancement depends on the echo time: Fig. 5b (short echo delay) exhibits a simple shift artifact at the shortest echo time. At longer echo times, the negative edge enhancement becomes more and more pronounced. Qualitatively, the negative edge enhancement may be understood by the following consideration: Without refocusing pulses, the signal attenuation of spins diffusing in a linear magnetic field gradient G for a time t is given as

$$\frac{S(t)}{S_0(t)} = e^{-(1/3)\gamma^2 G^2 D t^3}, \qquad [1]$$

with D denoting the diffusion coefficient, γ the gyromagnetic ratio ot the nuclei, $S(t)$ the signal intensity with diffusion, and $S_0(t)$ the signal intensity in the absence of diffusion (*13, 14*).

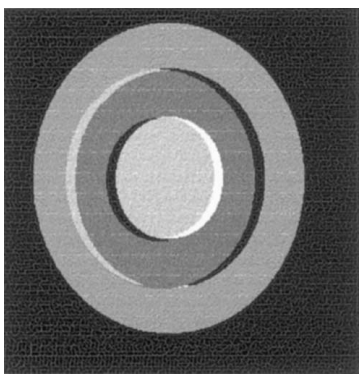

FIG. 3. Simulated image of the shift artifacts to be expected in an alginate tube partially loaded with paramagnetic ions.

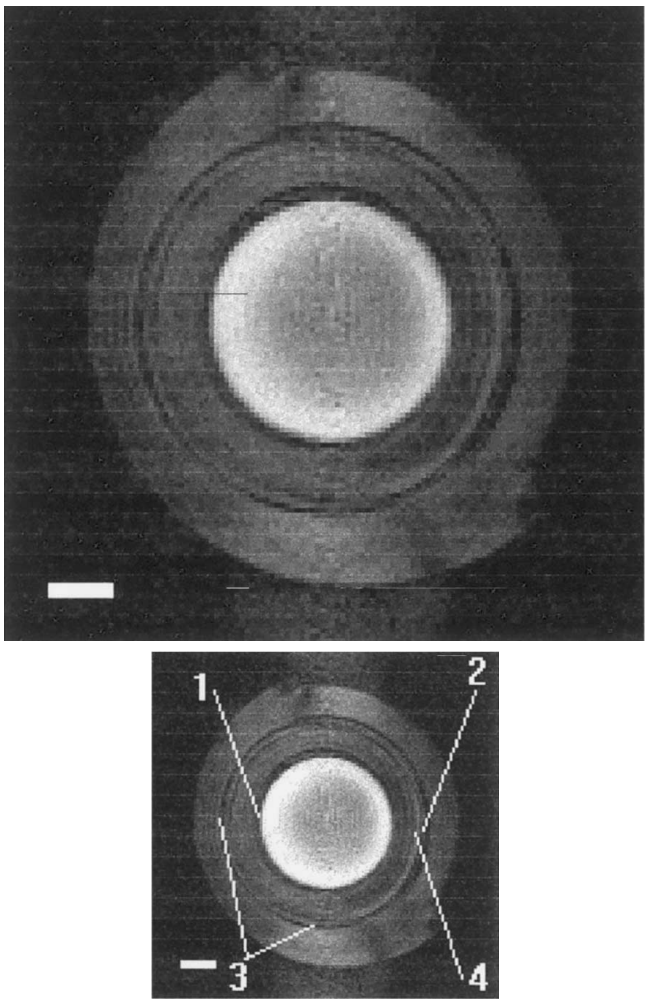

FIG. 4. Observed artifact structure in an alginate tube after 13 h loading with 1 mM Pr^{3+} at an echo time TE = 10 ms. The dark parts of the expected shift artifacts (marked 1 and 2 in the small picture) are clearly visible. Instead of the bright shift artifacts, a symmetrical dark line—the ''negative edge enhancement''—can be seen all around the sample (3). The additional structure marked with 4 is not a systematic one. It is probably due to a mirror artifact. The bright bar again corresponds to 1 mm.

Assuming that D is uniform and that the variation of the gradient is negligible on the length scale of the displacements, we may generalize

$$\frac{S(x, y, t)}{S_0(x, y, t)} = e^{-(1/3)\gamma^2 [G(x,y)]^2 D t^3}. \qquad [2]$$

As the susceptibility-induced gradient is particularly strong at the susceptibility interfaces (Fig. 6), strongly attenuated fringe patterns are expected wherever a susceptibility step without diffusion barrier occurs. Despite the crude assumptions on which Eq. [2] is based, it permits one to judge whether the observed artifacts can be accounted for as diffu-

sive attenuation in susceptibility-induced local field gradients: Assuming a front width of about 100 μm, a concentration difference of about 33 mmol/l and a molar susceptibility 5.5×10^{-9} m^3/mol for Pr^{3+} ions at room temperature, one can calculate the magnetic field gradient according to

$$\frac{dB(x)}{dx} = \frac{\chi_M}{3} \frac{dc(x)}{dx} B_0. \qquad [3]$$

For a 200 MHz (4.7 T) magnet, this leads to a gradient of about 35 mT/m. Based on Eq. [2], this gradient and a self-diffusion coefficient of water of 2.29×10^{-9} m^2/s and an echo time of 10 ms suggest a signal attenuation of about 20%. For an echo time of 12 ms, the attenuation is already increased to about 35%. These values for the attenuation are in a reasonable accord with the experimental findings.

To conclude, we have observed and characterized a new form of image artifact occurring in samples with a homogeneous diffusive propagator if susceptibility steps are present. Such steps are not limited to internal boundaries in polyelectrolyte gels and polyelectrolyte–water interfaces but they also should be observable in various biological samples at microimaging resolution. Further studies of the phenomena in phantoms made from polyelectrolytes might be helpful in order to gain a better understanding of the effects in more complex biological specimens. Polysaccharide samples have already been used for quite a long time in medical imaging (*15*). Most probably, the relatively big pixel sizes in such purely medical studies were the reason that negative edge enhancement was never observed in these experiments.

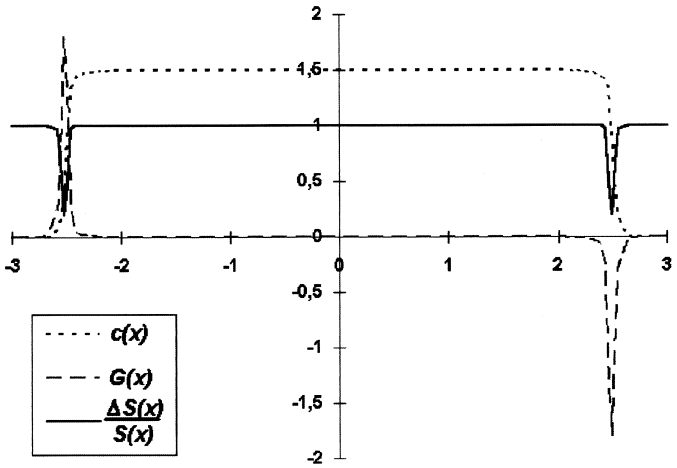

FIG. 6. Concentration profile $c(x)$, longitudinal component of the field gradient $G(x)$, and additional signal attenuation due to diffusion in the gradient $G(x)$ computed according to Eq. [2]. All quantities are in arbitrary units. One clearly can recognize the reduced signal intensity (i.e., the negative edge enhancement) at the edges of the concentration profile.

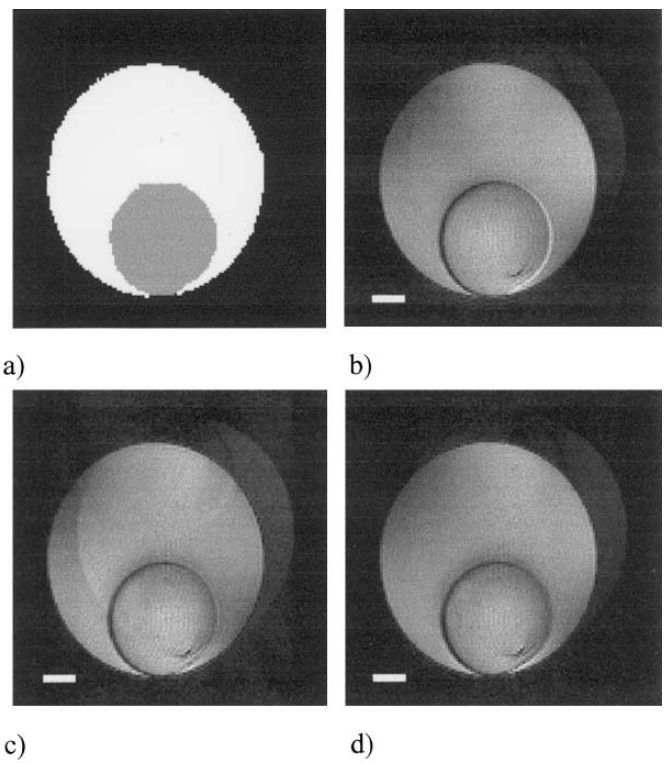

FIG. 5. Images of a sample consisting of a Ce-alginate cylinder immersed in water (a) at different echo times: (b) $T_E = 10$ ms, (c) $T_E = 12$ ms, (d) $T_E = 14$ ms. The bright bar again corresponds to 1 mm. Note the change in the artifact structure: while there is still the ''classical'' shift artifact at the shortest echo time, the negative edge enhancement is getting more and more prominent at longer echo times.

REFERENCES

1. W. B. Hyslop and P. C. Lauterbur, *J. Magn. Reson.* **94,** 501–510 (1991).
2. B. Pütz, D. Barsky, and K. Schulten, *J. Magn. Reson.* **97,** 27–53 (1992).
3. P. T. Callaghan, A. Coy, L. C. Forde, and C. J. Rofe, *J. Magn. Reson. A* **101,** 347–350 (1993).
4. M. Brandl and A. Haase, *J. Magn. Reson. B.* **103,** 162–167 (1994).
5. P. T. Callaghan, L. C. Forde, and C. J. Rofe, *J. Magn. Reson. B.* **104,** 34–52 (1994).
6. A. Haase, M. Brandl, E. Kuchenbrod, and A. Link, *J. Magn. Reson. A.* **105,** 230–233 (1993).
7. N. Nestle and R. Kimmich, *Heat Mass Transfer* **32,** 9–15 (1996). [In German]
8. N. Nestle and R. Kimmich, *Colloids Surf. A* **115,** 141–147 (1996).
9. N. Nestle and R. Kimmich, *Biotechnol. Bioeng.* **51,** 538–543 (1996).
10. N. Nestle and R. Kimmich, *Magn. Reson. Imaging* **14,** 905–906 (1996).
11. N. Nestle, thesis (CD-ROM), Universität Ulm, 1995.
12. L. Pavesi and A. Rigamonti, *Phys. Rev. E* **51,** 3318–3323 (1995).
13. E. L. Hahn, *Phys. Rev.* **80,** 580–594 (1950).
14. P. T. Callaghan, ''Principles of Nuclear Magnetic Resonance Microscopy,'' Clarendon, Oxford, 1991.
15. G. P. Mazzara, R. W. Briggs, Z. Wu, and B. G. Steinbach, *Magn. Reson. Imaging* **14,** 639–648 (1996).